Technical report; TR-193

KNMI

Error modelling of scatterometer, *in-situ*, and ECMWF model winds; A calibration refinement

Ad Stoffelen

De Bilt, 1996

Technical report = technisch rapport; TR-193

De Bilt, 1996

P.O. 30x 201
3730 AE De Bilt
Wilhelminalaan 10
Telefoon 030-220 69 11
telefax 030-221 04 07

ESA contract report;
contract no. RFQ/AOP/WK/333193

UDC: 551.507.362.2
551.501.75

ISSN: 0169-1708

ISBN: 90-369-2110-4

● ● ● ●

KNMI

European Space Agency Contract Report

Error modelling of scatterometer, *in-situ*, and ECMWF model winds; A calibration refinement

Author: Ad Stoffelen

ESA contract number: RFQ/AOP/WK/333193

Contents

Abstract

Wind is a very important dynamical variable to measure and satellites provide a unique capability to obtain such data with large spatial and temporal coverage. A statistical phenomenon important for the validation or calibration of winds is the small dynamic range relative to the typical measurement uncertainty, i.e. the generally small Signal-to-Noise Ratio. It can be more generally shown that in such cases *pseudo* biases may occur, when standard validation or calibration methods are applied, such as regression or bin-average analyses. Also, non-linear transformation, for instance between wind components and speed and direction, will generally give rise to *pseudo* biases. In fact, validation or calibration can only be done properly when the full error characteristics of the data are known. The problem is that in practise prior knowledge on the error characteristics is seldom available. Only by using triple collocations, error modelling and calibration of two of the systems with respect to the third may be achieved. In this report, *in situ,* scatterometer, and ECMWF model winds were used for this purpose. Wind component error analysis is shown to be more convenient than wind speed and direction error analysis. The *in situ* winds from real-time available buoys, fixed platforms, and a few other stations are shown to have the largest error variance, followed by the scatterometer, and the ECMWF model winds proved the most accurate. When using the *in situ* winds as a reference, surprisingly only the across-track wind component was biased low by 5 %, while the other component proved unbiased. Also, direction biases of the scatterometer with respect to the *in situ* and ECMWF model winds were demonstrated, but not explained. The ECMWF model winds are biased high by 6 % on both components for the period studied here. Further analysis, using more extended triple collocation data sets is recommended to confirm our conclusions.

1. Introduction

The current operational ERS scatterometer processing uses the transfer function CMOD4 to derive winds from the backscatter measurements. CMOD4 was derived with a Maximum Likelihood Estimation (MLE) procedure using ERS measurements and ECMWF analysis winds (operational winds in november 1991) as input (Stoffelen and Anderson, 1995). The transfer function was verified against winds from the ESA-led Haltenbanken field campaign, and winds from the global forecast model of the British Meteorological Office, UKMO, (Offiler, 1994), and selected as the preferable function amongst some other proposals. Winds from Numerical Weather Prediction (NWP) models are only a good reference, when they in turn are monitored against *in situ* winds from conventional platforms. Also, in a calibration exercise it is important that a representative sample of the day-to-day weather events is present. With hindsight, the Haltenbanken campaign was perhaps too limited in extend to guarantee this.

Furthermore, wind errors are generally large such that the Signal-to-Noise Ratio (SNR) is not negligible with respect to one (1). Then standard regression, curve fitting or bin average (BA) analyses may lead to substantial *pseudo* bias effects through an imperfect representation of the error characteristics of both reference and calibration systems. It will be shown here that only by using triple collocations and a profound error analysis such effects may be avoided. In this study we will use a one-year data set of triple collocations of anemometer winds operationally available at Méteó-France, scatterometer winds and ECMWF model winds. We will re-address the wind calibration of CMOD4.

1.1 Observation errors

In order to calibrate an observing system, we will need to have a good notion of what parameter we want to measure, i.e. what variable, but also on what temporal and spatial scale. The variable we will be comparing will be the vector wind at a height of 10 m above the ocean surface. We will ignore temporal effects and assume that all observing systems involved represent the same temporal scales. In the spatial domain, the *in situ* data represent a local estimate and will therefore be able to measure the wind variability on all scales. On the other hand, the scatterometer with a footprint of 50 km will not measure the variability on scales smaller than 50 km. The variability measured by an anemometer and not by the scatterometer is more generally indicated as representativeness error (see section 5).

For a detailed calibration a good notion of the accuracy of the observation systems is necessary, i.e. we need to know what may be called "the cloud of doubt" around the measurement. The nature and amount of system error has to be taken into account. Usually errors are classified as systematic (bias) or random (Standard Error; SE). For most observing systems one can distinguish detection errors and interpretation errors. The detection error includes measurement accuracy and digitizing effects, whereas the interpretation error is made when transforming the measurement(s) to the required variable(s).

For example for buoys the detection error is determined by anemometer characteristics and buoy motion. The interpretation error for anemometer winds has only to do with the correction (or the lack of it) of the measurements to a height of 10 m and with the collocation time and space window (see e.g. Wilkerson and Earle (1990) for a more detailed discussion).

For the scatterometer, the detection error is fairly small, and expressed in vector wind RMS roughly 0.5 ms^{-1} (Stoffelen and Anderson, 1995). On the other hand, the interpretation error is larger, and depends mainly on the accuracy of CMOD4 (the inversion error is small). The main cause is that CMOD4 does not contain effects such as stability, rain, and waves that are independent of the 10m wind. Backscatter effects that are correlated with the 10m wind will be included in CMOD4 and not contribute to the error of the scatterometer derived winds.

Although a model wind is not a measurement, it can be treated as an observation, since it contains information from all observations of mass and wind that were assimilated in the past. Its error will be largely independent from the errors of the current observations. The ECMWF model lowest model layer is approximately at 30 m. In a post-processing step 10 m winds are derived from model parameters. Errors here are caused by errors in the model state (dynamics) and by errors in the extrapolation module for the atmospheric boundary layer.

1.2 "True" state and pseudo *biases*

Unfortunately, all observation systems contain error. This means that we cannot assume that one measurement represents the true state, and calibrate the other against it, as we will illustrate here. Assume we have a distribution of "true" states, indicated by the variable t, with expected variance $\langle t^2 \rangle = \sigma^2$, and two independent measurement systems X and Y, indicated respectively by the variables x and y, with error variances of respectively $\langle (t-x)^2 \rangle = \varepsilon_x^2$ and $\langle (t-y)^2 \rangle = \varepsilon_y^2$. One can show that if the distribution of true values and the error distributions are normal that for fixed x the average of y does not lie at $\langle y \rangle = x$, but at $\langle y \rangle = \sigma^2 (\sigma^2 + \varepsilon_x^2)^{-1} x$ (see appendix A), i.e. for $\sigma = 5.$ ms^{-1} and a typical wind error of $\varepsilon_x = 2.$ ms^{-1} we find $\langle y \rangle = 0.84\ x$, which implies a 1.6 ms^{-1} difference at 10 ms^{-1}. So, for unbiased Gaussian error distributions, computing the mean of y for a fixed subrange or bin of x (bin average analysis) does in general reveal a *pseudo* bias that depends on the error characteristics of system X.

Scatterometer data are often verified against buoy data, where the buoy data are assumed to be "surface truth" (see e.g. Rufenach, 1995). We will show later, however, that the representativeness error for anemometer winds is substantial, and therefore this assumption does not hold. As such, in this work the observation error of *in situ* winds will be accounted for in the interpretation in order to be able to draw valid conclusions on the scatterometer bias.

A better assumption often used either implicitly (e.g. in "geometric mean" linear regression) or explicitly is $\varepsilon_y = \varepsilon_x$ leading to the expectation $\langle x^2 \rangle = \langle y^2 \rangle$. Again, for $\sigma = 5.$ ms^{-1} but now for the common wind errors of $\varepsilon_x = 3.$ ms^{-1} and $\varepsilon_y = 1.$ ms^{-1}, we find a ratio of the variances of $\langle x^2 \rangle \langle y^2 \rangle^{-1} = 1.32$ which would result in the conclusion that system Y is biased low by 16 %. Thus the assumption implies a 1.6 ms^{-1} *pseudo* bias at 10 ms^{-1} for in reality unbiased Gaussian error distributions. The examples illustrate that when a noisy system is used as a reference for

calibration, then we will need to know the error characteristics of that system. Further prove of this is given in appendix A.

Another possibility of generating *pseudo* bias is by non-linear transformation. An unbiased symmetric error distribution may then be transformed into a biased and skew error distribution. For example, Gaussian errors on the wind components u and v for system X or Y will not correspond to Gaussian error distributions on wind speed f and direction ϕ. Using the same notation and assumptions as in the previous two examples we show in appendix B that $< f_x > = \sqrt{\pi/2}\,\sigma_x$ where $\sigma_x^2 = \sigma^2 + \varepsilon_x^2$, with σ the standard deviation (SD) of the true distribution and ε_x the SE of system X, when the errors are identical for the u and v components. A similar expression can be derived for system Y. The expected mean wind speed difference will be $< f_x - f_y > = \sqrt{\pi/2}(\sigma_x - \sigma_y) \approx \sqrt{\pi/2}(\varepsilon_x^2 - \varepsilon_y^2)/\sigma$. For example, the typical values of $(\sigma, \varepsilon_x, \varepsilon_y) = (5., 3., 1.)$ will lead to an average wind speed bias of 0.4 ms^{-1}. This is a *pseudo* bias since the error in the wind components is unbiased. One can show that the *pseudo* bias generally oscillates from positive to negative as a function of wind speed and is relatively largest for low speeds (see figure 2).

It may be clear from the above that it is desireable that the error characteristics of measurement systems are well described, thereby avoiding corrections for *pseudo* bias effects only due to inaccurate assumptions on the errors. Furthermore, to provide a calibration and error model of observing systems it is also desireable that the error model is simple to describe, preferably avoiding statistical moments of order higher than two.

1.3 Overview

We addressed the problem of *pseudo* biases by studying the error characteristics of *in-situ*, scatterometer and ECMWF model winds through intercomparison. In section 2 we will discuss the selection of a measurement domain where the errors are simple to describe. *Pseudo* biases after non-linear transformation will also be further discussed The wind components rather than speed and direction are shown to be the most convenient to provide an accurate description of observation errors. Mean wind components are generally close to each other (zero) since both positive and negative values exist. The first order calibration problem we discuss is therefore a multiplication factor or scaling (a linear regression with zero bias term) that will for a particular true value t provide calibrated measurements x with expectation value $<x> = t$. In the case of intercomparison of two noisy systems it is without prior knowledge not possible to resolve both observation system error characteristics and calibration. In section 3 it is shown that with three noisy systems, it is possible to calibrate two of the systems with respect to the third, and at the same time provide an error characterisation for all three systems. We have used the *in-situ* winds as a reference and scaled the scatterometer and ECMWF model winds to have the same average strength. In section 4 a higher order, or more detailed, calibration is considered.

Using a climatological wind component spectrum we estimate the representativeness error of the scatterometer and *in-situ* data with respect to the ECMWF model in section 5. After discussing wind direction effects in section 6, section 7 provides the error model parameters and calibration

scaling factors. Sections 8 and 9 discuss the implications of this study for scatterometer data processing and wind data interpretation and assimilation.

2. Error domain

When trying to characterise measurement errors, it is practical to select a parameter domain where the "cloud of doubt" is simple to describe. When it is symmetric then first and second order statistical moments may be sufficient to describe the errors and simulate the measurements.

Although we need not to limit ourselves to these, for wind the two physical choices are either wind components (u,v), or wind speed and direction (f,ϕ). These are non-linearly related. We discussed in the introduction that random errors in the one domain may generate a serious *pseudo* bias in the other domain.

One way to approach error characterisation is to look in detail at the error sources. The anemometer characteristics for *in situ* winds will vary, but will generally not be the dominant error source. Interpretation errors, including height correction to 10m and platform motion correction errors, may be more substantial for the conventional winds, but some components of it are well characterised in the (f,d) domain, whilst other components are better characterised in the (u,v) domain. A major contribution to the observation error for conventional winds when comparing to scatterometer data or ECMWF model winds will be the representativeness error. As will be shown later in section 5, this part of the total observation error is well characterised in the wind component domain. Scatterometer winds are empirically derived and it is very difficult to assess which geophysical elements (e.g. waves, stability, rain, or sea surface temperature) determine the interpretation error. The error sources in the ECMWF model that project onto the surface wind are even more difficult to elaborate on. It may be clear that a characterisation of the total observation error from a quantification of all the error sources contributing to it will be undoable. Therefore, an empirical approach was adopted here.

In figure 1 the distribution of scatterometer winds for a fixed ECMWF model wind subdomain is shown, in both physical spaces. Since, the ECMWF model is not perfect, the subdomain of true winds will be larger than the subdomain of the model winds, i.e. it is clear that the shown distribution is effected by errors in both the ECMWF model and the scatterometer (see appendix A and note that $p(y|x) \propto p(x,y)$). We can see that the component errors are well-captured by a symmetric distribution (Gaussian). On the other hand the wind direction random error clearly depends on wind speed, i.e. the lighter the wind the larger the wind direction error. The wind speed error is not symmetrically distributed for light winds but skew, i.e. large positive errors are more likely than large negative errors (Hinton and Wylie, 1985). This is related to the fact that measured negative wind speeds can not occur.

Moreover, the "cloud of doubt" in the (f,ϕ) space is quite complicated and can not be described by second order statistics, whereas in (u,v) space the "cloud of doubt" seems much simpler to

describe. Therefore, as is common practise in meteorological data assimilation, we will define an error model in the wind components.

In practise it is found that the random error on both the u and v components is similar, as one may expect (see e.g. figure 1a). Also, by verifying the error distributions at higher speeds, we found little evidence of speed dependent component errors in the observation systems studied (see e.g. figure 2). Therefore, the error model with constant and normal component errors as used in the introduction is well suited. It implies for speed and direction that the expected RMS wind speed difference $<(f_x - f_y)^2>$ increases monotonically with wind speed, and the wind direction RMS $<(\phi_x - \phi_y)^2>$ increases monotonically to a value of 104 degrees for decreasing wind speed. Hinton and Wylie used a truncated Gaussian error distribution that did not allow negative speeds, to correct for the low speed *pseudo* bias. This procedure is rather unsatisfactory, since it is not likely that the true error distribution contains discontinuities. By assuming Gaussian error distributions in the wind components the cut-off speed effect is also simulated, thereby avoiding their *ad hoc* correction.

A good way to verify our approach is to simulate the wind speed and direction difference statistics with the error model we have obtained for the wind components. Figure 2 shows such a comparison. We can see that the average wind speed difference (*pseudo* bias) indeed varies as a function of wind speed, and that it can be as large as 1 ms^{-1}. The standard deviation of the wind speed difference and the vector RMS difference go to a small value for low wind speed, as is observed for the real data as well. The wind direction standard deviation increases for decreasing wind speed and goes to a value of a hundred odd, as expected (random direction). The wind direction bias is very small as should be. Thus, our error model is as well able to simulate the observed difference statistics in the wind components as the difference statistics in wind speed and direction, thereby confirming its adequacy.

3. Error modelling and calibration with three systems

In the introduction it was indicated that calibration of one noisy system against another is not possible without fundamental assumptions on the noise characteristics of at least one system. It was shown that these assumptions may lead to substantial *pseudo* bias problems. This is further elaborated in appendix A. Here a method will be introduced to perform calibration and error modelling using triple collocations. The method is quite general and will be introduced as such. Later on the method will be applied on *in situ*, scatterometer and ECMWF model wind components. Now suppose three measurement systems *X*, *Y* and *Z* measuring a true variable *t*. Let's define:

$$\begin{aligned} x &= t + \delta_x \;;\; \varepsilon_x^2 = <\delta_x^2> \\ y &= s_y(t + \delta_y) \;;\; \varepsilon_y^2 = <\delta_y^2> \\ z &= s_z(t + \delta_z) \;;\; \varepsilon_z^2 = <\delta_z^2> \end{aligned} \qquad (1)$$

with as before $\sigma^2 = <t^2>$, and now δ_x, δ_y and δ_z the random observation errors in respectively the measurements x, y, and z. s_y and s_z are the calibration (scaling) constants. The observation errors are assumed uncorrelated with t, i.e. $<\delta_x t> = <\delta_y t> = <\delta_z t> = 0$. We have assumed a zero the true distribution's mean and no systematic errors, i.e. $<t> = <\delta_x> = <\delta_y> = <\delta_z> = 0$. For marine winds this is valid to good approximation (see section 7).

It is unlikely that the three systems represent the same spatial scales. Therefore, we will arbitrarily assume that observation systems X and Y can resolve smaller scales than system Z by taking $<\delta_x \delta_y> = r^2$, which means that the smaller scales are part of the observation errors δ_x and δ_y, and that t only represents the spatial scales resolved by z. Since z does not resolve the smaller scales the observation error of system Z is independent of the errors of X and Y, i.e. $<\delta_x \delta_z> = <\delta_y \delta_z> = 0$. r^2 is the correlated part of the representativeness errors of X and Y. The assumption that the wind component errors of the different observation systems are uncorrelated, except for the representativeness error, is essential to determine the calibration. In some cases such an assumption may be unrealistic, but we believe that in our case this is realistic to good approximation. Now the calibration coefficients can be derived from the different covariances:

$$\begin{aligned} s_y &= <yz><zx>^{-1} \\ s_z &= <yz><zx>(<xy><zx> - r^2<yz>)^{-1} \end{aligned} \qquad \textbf{(2)}$$

These coefficients can be used to create $z^* = s_z^{-1} z$ and $y^* = s_y^{-1} y$, which are the calibrated data. Subsequently, all random error parameters of the observation systems X,Y and Z can be resolved pair-wise from the different covariances, as illustrated in appendix A by equation **(A5)**. Here we used observation system X as a reference system. This preference can be easily altered by scaling all parameters to one of the other systems. So, under the premise that we find an estimate for r^2 (see section 5) we have found a way to perform a first order calibration.

4. Higher order calibration

After the first order calibration, the three systems should be largely unbiased. However, in this section we will consider a more detailed calibration of the systems by pair-wise comparison. For the triple collocated data the procedure will be run comparing X and Y, Y and Z, and Z and X so that consistency can be checked between the results.

Now first consider X and Y. After obtaining ε_x and ε_y we decide which system is the least noisy, for example suppose $\varepsilon_x > \varepsilon_y$. Then system Y may be convoluted with a Gaussian distribution with width $\sqrt{\varepsilon_x^2 - \varepsilon_y^2}$ to obtain a distribution (and system Y') that has the same error properties as system X. In fact, since they also represent the same true distribution, the resulting distributions of X and Y' should be identical in case of a large sample size. By comparing the cumulative distributions of these two systems, respectively $f(x)$ and $g(y')$, that are monotonically increasing functions, we can easily compute a mapping $y^\mu = \mu(y)$ that results in identical

distributions $f(x)$ and $g(y^{\mu})$. The higher order correction would then be $\mu(y)$-y, which may be plotted versus y.

At first sight this seems a very powerful method that shows all bias problems. However, when we look at equation **(A1)** we readily see that the joint distribution of x and y does depend on the error properties of x and y and on the distribution of true values. In the procedure presented above, we have only considered second order statistical moments and their effect on bias. Higher order statistical moments in the error characteristics may have *pseudo* bias effects in some parts of the domain. These effects will remain present after the above mapping and therefore care should be taken in applying the mapping as a correction on either x or y. Also, at the extreme ends insufficient data may be present to warrant a reasonable estimate of the real bias. To gain confidence, the computed corrections may be verified by simulation or by a consistency check when more than two systems are involved, such as in our triple collocation data set.

5. Representativeness

Until this point the methodology has been quite general. However, to resolve the problem of representativeness, we have to look at the specific systems we are going to use. For the calibration of the scatterometer we will use *in situ* winds as the reference system (X). Furthermore, the observational system that has the lowest spatial resolution is the ECMWF model (Stoffelen and Anderson, 1995), which will be used as system Z. Observation system Y is therefore the scatterometer. The scatterometer has a footprint size of 50 km and as such a smaller spatial resolution than the *in situ* winds. In the previous section, in t was represented the spatial resolution of Z and r^2 represented the scales resolved by both X and Y, but not by Z. As discussed earlier, the variability on the scales resolved by the *in situ* data, but not by the scatterometer nor the ECMWF model, will be accounted for in the observation error of the *in situ* winds. This in turn means that r^2 represents the scales resolved by the scatterometer, but not by the ECMWF model. This brings us in a fortunate position, since we can easily study the effect of spatial averaging for the scatterometer and the ECMWF model in order to estimate the spatial representativeness of both systems.

5.1 Computation of r^2

Now, lets assume we compare two systems at a certain spatial resolution for which we define the error characteristics as before. Then, suppose we are able to compare the same two measurement systems at a different and higher resolution with true state $t + \tau$ for which $<\tau^2> = \Sigma^2$ and:

$$\begin{aligned} \xi &= a\tau + \partial_x \\ \psi &= b\tau + \partial_y \end{aligned} \qquad \textbf{(3)}$$

The higher resolution measurements $x+\xi$ and $y+\psi$ have additional error ∂_x and ∂_y, that represents the error when measuring the additional smaller scales. Further, we have assumed that

the smaller scales are only partially resolved, respectively fraction a and b for ξ and ψ. We want to resolve the representativeness error in the resolution range of τ which is given by:

$$r^2 = \left| a^2 - b^2 \right| \Sigma^2 \tag{4}$$

We again assume that the errors are mutually independent and that the errors are independent of the truth, but now at both spatial resolutions (of t and t $+\tau$). We also assume that the errors on the scale of t are independent of the errors on the smaller scales incorporated in τ. We now find for the covariances of both systems in the spatial range represented by τ:

$$\begin{aligned} I: &< (x+\xi)^2 > - < x^2 > \; = a^2\Sigma^2 + \mathrm{E}_x^2 \\ II: &< (y+\psi)^2 > - < y^2 > \; = b^2\Sigma^2 + \mathrm{E}_y^2 \\ III: &< (x+\xi)(y+\psi) > - < xy > \; = ab\Sigma^2 \end{aligned} \tag{5}$$

where $\mathrm{E}_x^2 = \; < \partial_x^{\,2} >$ and $\mathrm{E}_y^2 = \; < \partial_y^{\,2} >$. The difference between I and II is thus not a good measure of the representativeness error, since one system may have a larger error than the other system, i.e. $\mathrm{E}_x^2 \neq \mathrm{E}_y^{\,2}$. The bottom equation (*III*) represents the true variance resolved by both systems. We note that if one system is unable to resolve τ, i.e. for example a = 0, then we will not be able to distinguish between error variance and true variance for the other system, since in this case the correlation of ξ and ψ will be zero. The upper limit of the true variance is then given by the total variance (*II*), and the lower limit is r^2 = 0. The other extreme case is when one system is perfect, i.e. for example a = 1 and $\mathrm{E}_x^2 = 0$, then the representativeness error will be $r^2 = I - III^2\, I^{-1}$.

To solve the representativeness error there are still too many unknowns. We write $\mathrm{E}_x^2 = \alpha\, a^2\Sigma^2$ and $\mathrm{E}_y^2 = \beta\, b^2\Sigma^2$ without loss of generality. As a final assumption we state $\alpha = \beta$, such that $r^2 = III\sqrt{I\,II}\left| I^{-1} - II^{-1} \right|$. This is a somewhat arbitrary choise, but seems to be better than assuming one of the systems to be perfect, or for instance assuming that both systems have the same absolute error. In next subsection we will discuss some implications of this choice.

5.2 Results

Figure 3 shows the variance of the scatterometer and the ECMWF model, and the correlation of both, for resolutions between 50 and 250 km. Figure 3a shows the along-track ERS-1 component and figure 3b the across-track component which turn out to behave quite differently for the larger of these scales. The difference in variance between scatterometer and ECMWF model is generally larger for the along-track component (roughly north-south) and the ECMWF model appears to resolve this component to a smaller degree than its orthogonal (across-track) component. For the larger scales, the scatterometer, and the ECMWF east-west component show the same amount of variance as the climatological spectrum, giving confidence in their validity.

The representativeness error (at 50 km) is the same for both components and roughly equal to 0.75 m^2s^{-2}.

We compared the above results before and after application of the calibration procedure as set out in section 3 (see section 7), but found no relevant difference in the estimate of the representativeness error. In fact, the results in figure 3 are for the calibrated scatterometer and ECMWF model winds.

	u component	*v* component
Scatterometer error	1.21 ms^{-1}	1.14 ms^{-1}
ECMWF error	0.90 ms^{-1}	0.95 ms^{-1}
Scatterometer fraction	0.76	0.85
ECMWF fraction	0.54	0.69

Table 1: Estimates of the standard errors of the scatterometer and ECMWF error distributions for the along-track (u) and across-track (v) ERS-1 wind components on scales between 50 and 250 km. The lower two rows give the fraction of the "true" variance resolved by both systems on these scales. The total standard error integrated over all scales should be larger (see table 3).

Figure 3 may be used to compute the contribution to the error variance in the ECMWF model and the scatterometer of scales from 50 to 250 km. For the two systems this is respectively the difference between the thin dashed line and the thick grey solid line, and the difference between the thin dotted line and the thick black line at the resolution value of 50 km. The results are given in table 1. Later on (table 3) we will show that the estimates of the total ECMWF u and v component standard errors are 0.95 ms^{-1} and 0.86 ms^{-1} respectively, i.e. its variance roughly equals the error contribution of the scales studied here and no error would be present in scales larger than 250 km. As such, this represents for the smaller scales the most pessimistic view regarding the ECMWF model error and its resolved "true" variance. As a consequence it is the most optimistic view for the scatterometer in that the scatterometer resolved "true" variance is maximal and the error minimum (see equation **(5)**). By looking at synoptic charts Stoffelen and Anderson (1995) got the experience that the scatterometer well resolves the smaller synoptic scales, but that the ECMWF model has a lower resolution. Therefore a pessimistic view for the scatterometer would be $a = b$ with according to equation **(4)** $r^2 = 0$, leading for fixed $\Sigma^2 = 2.75$ m^2s^{-2} with equations **(5)** to $a = 0.66$ (*III*), $E_x = 1.36$ ms^{-1} (*I*) and $E_y = 0.63$ ms^{-1} (*II*) for the u component and $a = 0.76$, $E_x = 1.30$ ms^{-1} and $E_y = 0.77$ ms^{-1} for the v component. Later on (table 3) we will show that the estimates of the total scatterometer u and v component standard errors are 1.86 ms^{-1} and 1.65 ms^{-1} respectively and are well above the small-scale contributions computed in this section. Therefore, it seems reasonable to assume $0 \leq r^2 \leq 0.75$. Given the synoptic verification of scatterometer and ECMWF model winds, we will use the difference in true variance at 50 km in figure 3a and 3b as the representativeness error, i.e. $r^2 = 0.75$ m^2s^{-2}. The sensitivity of the results to this choice will be discussed later on and shown to be small (section 7).

The total scatterometer error variance is roughly twice the error contribution of the scales studied here and substantial error variance would originate from scales larger than 250 km. This would

imply some spatial error correlation in the scatterometer winds in contradiction to what was concluded by Stoffelen and Anderson (1995) on the basis of a simpler analysis.

6. Wind direction bias

We took some special care with directional effects, given our experience that the scatterometer and ECMWF model are slightly biased. Figure 4 shows this bias as a function of latitude. The meteorological definition of direction is used, which means that the northern hemisphere (NH) scatterometer wind direction is veered with respect to the ECMWF model wind direction, and in the southern hemisphere (SH) backed. Independent of whether passes are ascending or descending, we found that the bias is strongest at middle latitudes and of opposite sign in both hemispheres. Therefore, it is likely that the bias is of a geophysical nature rather than a technical problem (with the scatterometer).

Given the opposite sign in both hemispheres a likely explanation may be that the direction bias is caused by the extrapolation of ECMWF model winds down to 10 m and the sign would indicate that this extrapolation was too geostrophic (too little friction). However, we now find that the bias of the *in situ* (roughly from 25N-65N) wind direction with the scatterometer is 5.1 degrees and with the ECMWF model 1.1 degrees, which indicates that the scatterometer is in disagreement with the conventional winds and that the ECMWF extrapolation works fairly well in general.

Provided there is no technical problem with the conventional winds we are led to believe that the scatterometer wind direction is in error. The scatterometer backscatter is directly related to the surface roughness on cm-scales, and is as such probably closely related to the surface stress. This stress is related to the friction velocity, which in turn defines the wind profile in the lowest tens of meters of the atmosphere, i.e. the so-called surface layer (e.g. Holton, 1979 p. 106-107). In the surface layer the stress is assumed to remain constant with height and as a result wind direction and surface stress direction are identical. This theory does therefore not allow an explanation for the scatterometer wind direction bias.

It has been found that the stress vector is not aligned with the 10 m wind vector in case of longer waves travelling at oblique angles with the wind vector (Geernaert et al., 1993 and Rieder et al., 1994). A shift of the backscatter maximum toward the direction of the swell has been observed (Hauser, 1994). Such an effect would explain the bias (in the NH) when on average the swell direction is veered with respect to the wind direction. In the area of largest bias we will generally have westerlies and associated low pressure systems propagating eastward, such that in a majority of cases wind will back with time. However, longer waves will propagate at a different speed (depending on wavelength both faster and slower) than the low pressure systems and it is difficult at this point to speculate whether the relevant long waves will be veered or backed on average. Further investigation is needed to understand the scatterometer wind direction bias.

Geernaert (1988) reports on experimental evidence of stress-wind direction differences depending on heat flux, which was obtained in the North Sea. Since the heat flux is wind speed

dependent, one would expect that also the turning is wind speed dependent. We did however not find a wind speed dependence of the wind direction bias between scatterometer and ECMWF model, but generally a rather constant bias as a function of speed (see figure 2). Furthermore, according to the heat flux dependency, a majority of situations with unstable stratification would explain the bias. However, in practise one would expect neutral or stable conditions to prevail over the open ocean.

Figure 4 shows also a significant bias in the tropical convergence zone. Closer inspection (not shown) reveals that this bias is mainly located at the directions at which the prevailing equatorial easterlies are sampled for descending and ascending passes. The bias agrees with the finding of Bryan et al. (1996) that the ECMWF cross-equatorial meridional wind is too weak. Collocations with TOGA-TOA buoys may confirm this finding.

It is relevant to know the effect of wind direction bias on the wind component statistics we are going to perform. A small wind direction bias $\Delta\phi$ at a wind speed f has, integrated over all wind directions, an effect on the wind component variance of:

$$\Delta u^2 \approx 0.5 f^2 \Delta\phi^2 \qquad \textbf{(6)}$$

A bias of 5 degrees at 10 ms^{-1} would according to equation **(6)** result in $\Delta u^2 \approx 0.4$ m^2s^{-2}, which is only a small effect. Nontheless, we corrected wind direction biases relative to the *in situ* winds, but indeed with negligible effect on the wind component statistics.

7. Calibration and error model results

In this section we show the results of the calibration of scatterometer and ECMWF winds relative to the anemometer winds. The real-time available anemometer winds were obtained from Météo-France, but also screened by the ECMWF monthly updated blacklists. The reports have not been checked for proper height corrections and just over 50 % of the reports arrived from the WMO station identifiers 63111, 62112, 62118, and 62122, which are platforms located in the North Sea. The scatterometer data were processed at ECMWF with PRESCAT (Stoffelen and Anderson, 1995). The ECMWF winds were from the First Guess at Appropriate Time (FGAT), which means that for each wind component a cubic time interpolation has been performed between a 3, 6, and 9 hour forecast to the time of observation of the scatterometer. The spatial interpolation of the forecasts to the scatterometer node is bi-linear in the wind components. The anemometer wind is within 3 hours and 100 km from the scatterometer measurement time and node respectively.

The average wind components of the *in situ* winds, scatterometer and FGAT are very close (within a few tenths of a ms^{-1}). As such, the assumption just below equation **(1)** that the systems have no absolute bias, i.e. $<\delta_i> = 0$, proves valid. A quality control procedure is applied to exclude gross errors. An iterative scheme is followed where in each trial a calibrated (see below

equation (2)) collocation triplet is rejected when for any pair the following condition holds, illustated here for pair (x,y^*):

$$|x - y^*| > 3\sqrt{\varepsilon_x^2 + \varepsilon_y^2} \qquad (7)$$

where the calibrations and the errors are taken from the previous trial. In the first trial we start with calibration factors equal to one and errors equal to 2 ms^{-1}. The calibration factors are within a percent of their final value after one iteration and also the rejection rates remain constant (at ~1%) after 1 or 2 trials; 6 trials were used. The wind direction bias correction is repeated after every trial, and the resulting corrections are 5.1 degrees for the scatterometer and 1.1 degrees for the ECMWF model, where the incremental correction in the sixth trial was very small (< 0.01 degrees).

7.1 First order calibration

The resulting calibration scaling factors are shown in table 2. Remarkably, the scatterometer along-track component is not biased, whereas the across-track component is biased by 5 % (too low). This result is very striking, since it implies a wind direction dependent speed scaling; in directions upwind and downwind to the mid beam speeds need to be upscaled and at crosswind they need to remain the same. The wind direction change implied by this calibration is quite small and at maximum 1.4 degrees at angles under 45 degrees with upwind, downwind and crosswind.

	u component scaling	v component scaling	r^2 [ms^{-1}]
Scatterometer	1.00	0.95	0.50
Scatterometer	1.00	0.95	0.75
Scatterometer	1.00	0.95	1.00
ECMWF FGAT	1.06	1.05	0.50
ECMWF FGAT	1.06	1.06	0.75
ECMWF FGAT	1.07	1.07	1.00

Table 2: Calibration scaling factors for the along-track (u) and across-track (v) wind components from the scatterometer and ECMWF model for different representativeness errors r^2 (due to scatterometer-FGAT spatial resolution difference).

The representativeness error estimate only influences the calibration coefficient of the ECMWF model as we would expect from equation (2), where its effect is only modest. ECMWF FGAT winds seem to be biased high with respect to the anemometer winds (by ~6 %). However, the calibrations may be influenced by improper anemometer height corrections and a platform identifier dependent height correction procedure is necessary to obtain a more precise result. It is noteworthy that CMOD4 was obtained by fitting it to the operational ECMWF model in november 1991 (Stoffelen and Anderson, 1995). This calibration shows that the ECMWF model winds have become stronger since that time.

Figure 5 shows the joint distributions of the wind components of *in situ* and scatterometer, scatterometer and FGAT, and FGAT and *in situ* data. It is evident that the scatter in the scatterometer and FGAT plot is smallest. This means that the *in situ* winds have the largest error. The *in situ* and scatterometer plot shows the largest scatter, which indicates that the FGAT winds are the most accurate. Table 3 shows the results of our random error estimates from equation **(A5)** in appendix A, which confirm our subjective analysis.

The error estimates for the u and v component are quite similar for all systems, but compare best for the conventional winds. We further note that in general the errors on the v component are slightly smaller than the errors on the u component for some reason.

In table 1 we estimated the ECMWF and scatterometer error contribution from scales between 50 and 250 km by comparison of the "true" resolved variance and the measured variance. The scatterometer contribution to the total standard error of 1.3 ms^{-1} and the FGAT contribution of 0.9 ms^{-1} for both the u and v components corresponds reasonably well to the error estimates in table 3. For FGAT it would implicate that the random error on scales larger than 250 km is small. However, for the scatterometer this error would be slightly over 1 ms^{-1} for both wind components and not negligible.

	u component $[ms^{-1}]$	v component $[ms^{-1}]$	r^2 $[m^2s^{-2}]$
True variance	6.70	6.53	0.75
In situ error	2.65	2.58	0.75
Scatter. error	1.86	1.65	0.75
ECMWF error	0.95	0.86	0.75

Table 3: Estimates of the standard deviation of the true distribution and the standard errors of the *in situ*, scatterometer and ECMWF distributions for the along-track (u) and across-track (v) ERS-1 wind components. The values are computed at the spatial representativeness of the ECMWF winds.

After estimating the representativeness error variance of the conventional winds with respect to FGAT to be 2.1 m^2s^{-2} from the climatological spectrum used in figure 3, then the (local) error of the *in situ* winds may be estimated as 2.20 ms^{-1} for the u and 2.13 ms^{-1} for the v component. Since the *in situ* winds are not exactly collocated in space and time with the scatterometer and FGAT winds, a collocation error could further be subtracted from the former. Wind measurements separated by in between 2 and 3 hours will have an additional error component of approximately 1.5 m^2s^{-2} (Stoffelen and Anderson, 1995). When we assume that the collocations are randomly distributed in time (over 6 hours), than the average error contribution is roughly 0.75 m^2s^{-2}. The spatial cut-off will not be a problem since we have done the estimates at a coarse resolution (of FGAT). When we subtract the collocation error (0.75 m^2s^{-2}) from the conventional data local error estimate the error is reduced from 2.20 and 2.13 ms^{-1} to 2.02 and 1.95 ms^{-1} for the u and v components respectively. However, the local wind is not as relevant for meteorological analysis and forecasting as an area-averaged quantity, such as from the scatterometer.

The scatterometer may well resolve scales smaller than 100 km, as discussed in section 5, and these would only partly verify with the anemometer wind measurements, given the collocation distance cut-off. This means that their correlation $r^2 = <\delta_x \delta_y>$ may be slightly overestimated due to the lax collocation constraints of the data set.

7.2 Higher order calibration

The higher order bias calibration procedure of section 4 requires a convolution of the most accurate system with a Gaussian error distribution with a width determined by the difference in error variance of the two systems. Figure 6 shows the higher order calibration by the cumulative distribution mapping method discussed in section 4. The biases appear to be rather random in nature. The smallest biases are generally present at small wind component values, and the highest at high component speeds. This is due to the fact that the largest number of data is present at low component speeds, and the lowest number at high speeds. In an attempt to fit the bias with a smooth function this would have to be taken into account, and changes at the tail of the distribution should be kept small. Besides this, one would probably also want some symmetry in the calibration for positive and negative values and consistency between the calibration pairs. This would limit the choice of fitting functions.

Inconsistency of the biases between the calibration pairs is most noticeable at the tail of the distributions, i.e. for example the bias of the *in situ* winds with respect to the scatterometer is not equal to the sum of the biases of the conventional winds with respect to FGAT and the bias of FGAT with respect to the scatterometer. Moreover, the plot suggests that the scatterometer has a generally negative bias with respect to the anemometer winds and FGAT for the along-track component. However, this effect is not confirmed by the differences in mean value of the scatterometer along-track component. Closer inspection reveals more (but smaller) inconsistencies. These indicate insufficient sample size or higher order statistical moments in the error distributions than those accounted for.

We note from figure 5 that the joint distributions are in general not very smooth, and a larger data set would be needed to achieve a more smooth result. The statistical effect of this undersampling may result in a *pseudo* bias in figure 6. To illustrate this, figure 7 shows the biases for three simulated observation systems with a Gaussian error with zero mean and standard errors of 2.6 ms^{-1}, 1.8 ms^{-1}, and 0.9 ms^{-1} for respectively the anemometer winds, scatterometer and FGAT. The original distribution and sample size of FGAT was taken to be the "true" distribution. We note that the biases, especially at the extreme ends, are quite large and comparable to those in figure 6

In figure 7 the "cloud of doubt" is assumed to be Gaussian with a fixed standard error. However, in reality, also here higher order moments may be relevant. Furthermore, the standard error may depend on the geophysical condition, for instance on stability, and we would need a representative sample of all these conditions. As such, the number of samples we need to determine the overall standard error may be quite large. Since there is no mechanism to remove the *pseudo* biases due to sampling and higher order moments, we do not believe there is ground

to perform a fitting procedure to remove the remaining (physical) bias. Of course, a larger triple collocation data set would be of help to overcome the sampling problem.

8. Corrections to the processing

8.1 Scatterometer wind retrieval

The necessary correction to the processing of scatterometer winds implies a different scaling of the wind components along and across the satellite propagation direction. It was found earlier that the triplet of backscatter measurements can be described by two parameters at each node. This was concluded from the fact that the triplets lie close to a two dimensional cone surface in the three dimensional measurement space (Stoffelen and Anderson, 1995). Now, we suggest to change the scalings of the parameters describing the surface. This means that a triplet backscatter vector, denoted σ_i^0 with $i = (1,2,3)$, originally assigned to a certain wind *(u,v)* will be assigned to a new wind *(u*,v*)* after the calibration, i.e. $\sigma_i^0 = f_i(u,v) \quad = f_i(u*/s_y^u, v*/s_y^v) = f_i*(u*,v*)$. This change is easily implemented in the scatterometer processing by performing the original inversion resulting in the CMOD4 winds *(u,v)*, and then re-scaling to the final wind *(u*,v*)*.

The inverse, however, is more complicated. For the mid beam the calibration is different along and across the beam, but for the fore and aft beam the calibration is defined with respect to a coordinate system at an angle of 45 degrees with the beam. As a consequence, f_i * is beam dependent. This may occur when the processing of backscatter for the mid beam is slightly different from the processing of the fore and aft beams, resulting in a corresponding slight difference in absolute sensitivity of backscatter to wind for given incidence angle.

However, for an identical processing, a beam look angle independent transfer function should exist, that effectively results in the same wind component scaling. However, given the complexity and non-linearity of the backscatter-to-wind relationship, it is not trivial to analytically derive such a function from the scatterometer wind calibration proposed in this work. It is proposed to scale a large distribution of winds with the calibration factors here obtained to the current CMOD4 wind level, then use CMOD4 to simulate backscatter values for all three beams, and finally use the estimation procedure as set out by Stoffelen and Anderson (1995) on the original winds and the simulated backscatter to obtain the coefficients of a calibrated transfer function (CMOD5).

8.2 Data assimilation

It is essential that NWP models assimilate unbiased data. The 6 % bias we found may result from physical parameterizations that also control atmospheric boundary layer humidity, depth and temperature, and that require careful tuning. Such biases, if detected, are therefore not easily corrected. It has been observed by ECMWF that the scatterometer bias with respect to the

ECMWF model as found here had the tendency to slow down the forecast winds in the analysis, and subsequently fill in low pressure systems. This effect can be circumvented by a FGAT wind correction to match the mean observed wind (Roquet and Gaffard, 1995). In the long term the FGAT bias correction should be replaced by forecast model improvements. The same strategy should be adopted for other analysis variables. A careful statistical error analysis as described in this work was shown to be essential to arrive at a proper bias correction.

Given the resolution of NWP models it is not worthwhile to assimilate scatterometer data at full resolution. Instead, since scatterometer data have higher resolution, some averaging may be applied before assimilation. However, in order to avoid horizontal error correlation, it is suggested not to use all nodes, e.g. assimilate one wind for every 16 nodes which is the average of the centre 4 nodes. It has been shown that (unknown) spatial error correlation in data may lead easily to erroneous analysis (e.g. Homleid et al, 1995).

High resolution forecast models are designed to predict more true variance. In the absence of high resolution observational input they will then certainly also produce more error variance. The RMS difference of observed minus forecast wind may therefore become larger, even when the smaller scales are better resolved. We have shown a way to verify such models against observations and a possibility to study improved representativeness of smaller scales (replace scatterometer with high resolution model, and ECMWF by degraded model).

9. Conclusions and recommendations

In order to calibrate one observing system with respect to the other, one may use, either explicitly or implicitly, a simplifying assumption on the errors of the two systems. For instance, it is common practise to assume that the errors of two systems that are compared are equal, or to assume that one system is much more accurate (i.e. is "truth") than the other. Given our results in table 3 and figure 2, it is obvious that both of these choices would have been crude. In the introduction we have shown that such assumptions may lead to substantial *pseudo* bias effects. In appendix A it is shown that it is impossible to calibrate one noisy system against another without such an assumption or other prior knowledge on the error characteristics of one or both systems. For a proper calibration of an observing system a reference system is necessary and at least one other observation system, that together can provide triple collocations.

It was found that the selection of a simple measurement domain where second order statistics are sufficient to describe the uncertainty of the measurements is preferred. More specifically, we have shown that wind error modelling using wind components is much simpler than error modelling using speed and direction. Errors in speed are asymmetric and direction errors are strongly speed dependent for light winds. By assuming constant and Gaussian wind component errors these features are well modelled, and it would on the other hand be quite complex to describe them in terms of speed and direction. Thus, wind component error statistics represent a simple method to describe complex errors in speed and direction.

We have shown that substantial *pseudo* wind speed biases can occur through the non-linear transformation of unbiased wind component errors to the wind speed and direction domain. In a

direct wind speed calibration, where usually unjustly symmetric error distributions are assumed, the *pseudo* biases would be taken out, leading to biased wind components (see also Hinton and Wylie, 1985). Wind component error modelling as proposed here elegantly solves this problem.

A method to calibrate noisy systems has been developed using triple collocations. Furthermore, in a pair-wise comparison of the observation systems, the covariances were used to estimate the true variance resolved by both systems and error variance of the observations.

After the calibration and the estimation of the observation errors, a more refined bias estimation procedure may be adopted. However, care has to be taken with the effects of sample size and higher order (than two) statistical moments of the error distributions. On the basis of a simulation of the effect of sampling, it was decided for our data set to only use the refined method results as an indication of the accuracy of the former first order calibration. Over larger data sets one may fit higher order curves to calibrate either the scatterometer or ECMWF model. However, at the tail of the distribution (high wind speeds), the sampling is by definition poor and only linear corrections are recommended.

Of all conventional surface wind observation systems the set of *in situ* winds used here compares best to the ECMWF model in routine operational verifications. Therefore we used these anemometer winds as a reference, although they turned out to be the least accurate amongst the scatterometer and ECMWF model winds. Also, the set used here suffers from the problem of improper height correction, which may bias the results. The usefullness of the triple collocation data set could be improved by a station to station height correction scheme and quality monitoring scheme. Alternatively, the procedure in this report could be repeated with an off-line NOAA buoy data set (see e.g. Wilkerson and Earle, 1990).

We found that the CMOD4-derived scatterometer winds are biased low by 5% on the component along the mid beam direction, but are not biased on the other component. This essentially means that the wind speed bias is wind direction dependent. The effect of the component scaling on wind direction is fairly small. For the time being, we propose to perform the component calibration after the inversion. The algorithmic implementation would just take output wind speed and direction, convert to along- and across-beam components, apply the calibration, and convert back to speed and direction. The derivation of a revised transfer function (CMOD5) incorporating the wind calibration could be achieved by putting simulated data in a Maximum Likelihood Estimation procedure (Stoffelen and Anderson, 1995) re-estimating the coefficients of CMOD4. However, further evaluation of the significance of the implied difference in backscatter-to-wind sensitivity of the mid beam and the fore and aft beams should take place first.

Investigation of wind direction biases revealed a scatterometer wind direction bias with respect to the *in situ* winds and the ECMWF model. Assuming no technical problem with the conventional data, this bias can not be explained by current backscatter and atmospheric boundary layer theory. Also, earlier experimental evidence of stability and/or wave effects seems not particularly consistent with our findings and further investigation seems worthwhile. The collocation of the ECMWF atmospheric and wave (WAM) model output with the scatterometer measurements, as currently realised at ECMWF, may be useful in this respect.

The ECMWF model appears to be very accurate, but biased high by 6 % for the period we examined ('94). The north-south wind component has apparently lower resolution than the east-west component (see figure 3). Our estimate of the spatial resolution of the east-west component (150 km) seems optimistic with respect to the spatial error correlation used in the ECMWF data assimilation scheme (250 km). The error in the ECMWF model is determined by an extrapolation error and a dynamical error. Given the fact that the scatterometer minus FGAT statistics are very similar in both hemispheres (not shown), and that the dynamical errors are known to be larger in the SH, we conclude that the largest error contribution is from the extrapolation. For data assimilation and data use purposes, a monitoring of ECMWF model marine wind speed biases is essential.

Tropical wind analysis is very important for ocean circulation models, and as such for the study of the earth's climate. We noted a large directional inconsistency between scatterometer and FGAT wind direction at the equator. The TOGA-TOA buoys may prove a relevant data set to enhance our knowledge of the utility of scatterometer and ECMWF winds in this area using the procedure described here.

Acknowledgements

This work has been greatly stimulated by discussions in the ESA ASCAT SAG. Herve Roquet provided me with the collocation data set. Gratitude for Evert Attema who critically reviewed this report.

References

Bryan, Frank O., Ilana Wainer, and William R. Holland, "Sensitivity of the tropical atlantic circulation to specification of wind stress climatology", J. Geoph. Res. -Oceans, paper 95JC02499, in press for 1996.

Geernaert, Gerald L., "Temporal and spatial variability of the wind stress vector", in "Radar scattering from modulated wind waves", eds. G. J. Komen and W. A. Oost, Proceedings of the workshop on modulation of short wind waves in the gravity-capillary range by non-uniform currents, held in Bergen aan Zee, The Netherlands, 24-26 May 1988, published in 1989, Kluwer, Dordrecht, the Netherlands, 273 p.

Geernaert, G. L., F. Hansen, M. Courtney, and T. Herbers, "Directional attributes of the ocean surface wind stress vector", J. Geoph. Res. 98, pp.16571-16582, 1993.

Hauser, D., "Relationship between the direction of friction velocity and the direction of wind in various sea-state situations observed during the semaphore campaign, Proceedings 2nd int. conf.

on air-sea int. and on meteo. and ocean. of the coastal zone, Lisbon, Portugal, 22-27 Sept., 1994, published in 1995 by Am. Meteor. Soc., pp. 257-258.

Homleid, Mariken, Lars-Anders Breivik, "Preparations for the assimilation of ERS-1 surface wind observations into numerical weather prediction models", Tellus 47A (1), pp. 62-79, 1995.

Hinton, Barry B., and Donald P. Wylie, "A correction for the errors in ship reports of light wind", J. Atm. Ocean. Techn. 2, pp.353-356, 1985.

Holton, James R., "An introduction to dynamic meteorology", Third edtion, Int. Geoph. Series - volume 23, ISBN 0-12-354360-6, Academic Press Inc. Ltd., London, 1992.

Offiler, D., "The calibration of ERS-1 satellite scatterometer winds", J. Atm. Ocean Techn. 11 (4), pp.1002-1017, 1994.

Rieder, K. F., J. A. Smith and R. A. Weller, Observed directional characteristics of the wind, wind stress and surface waves on the open ocean", J. Geoph. Res. 99, pp.22589-22596, 1994.

Roquet, Hervé and Catherine Gaffard, "Proposal for a new version of CMOD4", ECMWF Research Department Memorandum; file R57.5.2/HR/57, 28 februari 1995, made available to the members of the ESA ASCAT SAG on 17 March 1995.

Rufenach, C., "A new relationship between radar cross-section and ocean surface wind speed using ERS-1 scatterometer and buoy measurements", Int. J. Remote Sensing 16, No. 18, pp. 3629-3647, 1995.

Stoffelen, Ad, and David Anderson, "The ECMWF contribution to the characterisation, interpretation, calibration and validation of ERS-1 scatterometer backscatter measurements and winds, and their use in numerical weather prediction models", ESA contract report and executive summary for contract 9097/90/NL/BI, published by ECMWF, Shinfield Park, Reading, Berkshire, UK, 1995.

Wilkerson, John C., and Marshall D. Earle,"A study of differences between environmental reports by ships in the voluntary observing program and measurements from buoys", J. Geoph. Res. 95 (C3), pp.3373-3385, 1990.

Appendix A: The necessity of error modelling before calibration or validation

In this appendix the problem of calibration and validation of one noisy system with respect to another one will be discussed. Usually scatter plots will be used to compare the data followed by a regression analysis to compute a calibration coefficient or to validate the system(s). The interpretation of scatter plots and associated regression and Bin Average (BA) analyses will be discussed, and it will be illustrated that calibration or validation, without knowing the error characteristics of one or both systems can easily lead to *pseudo* biases. In the second part, it will be illustrated that calibration or validation of one noisy system against another, without knowing the error characteristics of the observing systems, is generally not possible.

A.1 Scatter plots and regression

Usually, a scatter plot is used to determine the error characteristics of a measurement system (see for example figure 4). Here, we quantify the properties of the scatter plot. When enough collocation data are available, then the density of points in the scatter plot is proportional to $p(x, y)$, the joint probability density of x and y. One can show that:

$$p(x, y)\, dxdy = \int p(x|t)\, p(y|t)\, p(t)\, dt\, dxdy \qquad \textbf{(A1)}$$

where we integrate over the distribution of "true" states $p(t)$, and $p(x|t)$ is the conditional probability density of x given t, which includes all measurement and error characteristics of the measurements x. (It is closely related to what was introduced as the "cloud of doubt" around observation x, which formally reads $p(t|x)$ and $p(t|x)\, p(x) = p(x|t)\, p(t)$). We can see that the joint distribution of x and y is not only determined by the error characteristics of both systems, but also by the distribution of "true" states. In the simple case of unbiased Gaussian errors and a RMS equal to ε_x or ε_y, and a Gaussian "true" distribution with zero mean and RMS σ, the joint probability density of x and y can be written as:

$$p(x, y) \propto \exp\left[-\frac{(\sigma^2 + \varepsilon_y^2)x^2 + (\sigma^2 + \varepsilon_x^2)y^2 - \sigma^2 xy}{2(\sigma^2\varepsilon_x^2 + \sigma^2\varepsilon_y^2 + \varepsilon_x^2\varepsilon_y^2)}\right] \qquad \textbf{(A2)}$$

For given x, the mean y value of this distribution does not lie at $y = x$, but at $y = \sigma^2(\sigma^2 + \varepsilon_x^2)^{-1} x$. So, even for unbiased Gaussian error distributions, computing the mean of y for a fixed subrange or bin of x (bin average) does in general reveal a *pseudo* bias that depends on the error characteristics of x. This needs to be accounted for in the interpretation, and therefore when correcting for bin average biases with respect to a reference system, the error characteristics of that system, in this case ε_x, need to be known well.

For calibration or validation often linear regression is used as a tool. For a well-calibrated system and in case of $\varepsilon_x = \varepsilon_y$, a "geometric mean" linear regression on the joint distribution would indeed result in the line $y = x$, but in the more general case of $\varepsilon_x \neq \varepsilon_y$ in $y = (\sigma^2 + \varepsilon_y^2)(\sigma^2 + \varepsilon_x^2)^{-1} x$, where it would again result in a *pseudo* bias. When the error characteristics of x and y are known a weighted fit may result in a proper calibration. However, most often the errors are unknown.

A.2 The necessity of error modelling before calibration

Then the question emerges: is it possible to perform a calibration or validation of one noisy system against the other without prior information on the error characteristics of one or both of the systems. Below we illustrate that this is generally not possible.

Suppose we have a set of true states, indicated by variable t, measured by systems X and Y resulting in measurements x and y. We define $\sigma^2 = < t^2 >$, where $< >$ denotes the expected mean, and introduce the error model:

$$\begin{aligned} x &= t + \delta_x \; ; \quad \varepsilon_x^2 = < \delta_x^2 > \\ y &= t + \delta_y \; ; \quad \varepsilon_y^2 = < \delta_y^2 > \end{aligned} \qquad \textbf{(A3)}$$

where x, y, t are as defined before and δ_x, δ_y are the independent observation errors on respectively x, y, i.e. $< \delta_x \delta_y > \approx 0$. The observation errors are random and uncorrelated with t, i.e. $< \delta_x t > \approx 0$ and $< \delta_y t > \approx 0$. We have removed the true distribution's mean and assumed no systematic errors, i.e. $< t > = 0$, $< \delta_x > = 0$, $< \delta_y > = 0$. This proves a valid assumption for marine wind components (see section 7). We now find:

$$\begin{aligned} < x^2 > &= \sigma^2 + \varepsilon_x^2 \\ < y^2 > &= \sigma^2 + \varepsilon_y^2 \\ < xy > &= \sigma^2 \end{aligned} \qquad \textbf{(A4)}$$

which are three equations with three unknowns that are easily resolved:

$$\begin{aligned} \varepsilon_x^2 &= < x^2 > - < xy > \\ \varepsilon_y^2 &= < y^2 > - < xy > \\ \sigma^2 &= < xy > \end{aligned} \qquad \textbf{(A5)}$$

Thus, from the covariances we can resolve the true variance and the standard errors of systems X and Y.

Now suppose that one system is not calibrated, for example we change equation **(A3)** to:

$$
\begin{aligned}
x &= t + \delta_x \; ; \quad \varepsilon_x^2 = \langle \delta_x^2 \rangle \\
y &= s_y(t + \delta_y) \; ; \quad \varepsilon_y^2 = \langle \delta_y^2 \rangle
\end{aligned}
\tag{A6}
$$

where s_y is the calibration (scaling) constant. We now find:

$$
\begin{aligned}
\varepsilon_x^{*2} &= \langle x^2 \rangle - \langle xy \rangle = \varepsilon_x^2 + (1 - s_y)\sigma^2 \\
\varepsilon_y^{*2} &= \langle y^2 \rangle - \langle xy \rangle = s_y^2 \varepsilon_y^2 + s_y(s_y - 1)\sigma^2 \\
\sigma^{*2} &= \langle xy \rangle = s_y \sigma^2
\end{aligned}
\tag{A7}
$$

such that for $\varepsilon_x^{*2} \geq 0$ and $\varepsilon_y^{*2} \geq 0$ the transformed distribution of $t^* = \sqrt{s_y}\, t$ in combination with error model:

$$
\begin{aligned}
x^* &= t^* + \delta_x^* \; ; \quad \langle \delta_x^{*2} \rangle = \varepsilon_x^{*2} \\
y^* &= t^* + \delta_y^* \; ; \quad \langle \delta_y^{*2} \rangle = \varepsilon_y^{*2}
\end{aligned}
\tag{A8}
$$

is statistically identical to the system defined in equation **(A3)**. Consequently, one can show that substituting the transformed quantitities defined in equations **(A7-8)** into equation **(A2)** rather than the real quantities of equation **(A3)** leads to an identical joint distribution. As such the calibration coefficient cannot be resolved unambiguously without further information on the errors in this general case.

This is due to the fact that we have three independent statistical variables, i.e. $\langle x^2 \rangle$, $\langle y^2 \rangle$, and $\langle xy \rangle$, and four unknowns that are $s_y, \sigma, \varepsilon_x, \varepsilon_y$, which leaves one degree of freedom. The constraint that the error variances need to be larger than zero allows the following values for the scaling constant s^*_y in case of $s_y = 1$. : $-\varepsilon_y^2(\sigma^2 + \varepsilon_y^2)^{-1} \leq s_y^* - 1 \leq \varepsilon_x^2 \sigma^{-2}$. Only the addition of an independent third system can help determine the unique and correct value.

Appendix B: Pseudo bias through non-linear transformation

A statistical problem, that is relevant for considering the optimal error domain, may occur through non-linear transformation. This is easily shown for wind speed f, that depends in a non-linear manner on the wind components (u,v). As an alternative to Hinton and Wylie (1985), we assume normal distributed errors on the wind components u and v for measurement systems X and Y, i.e. $u_x = N(u_t, \varepsilon_x)$, $v_x = N(v_t, \varepsilon_x)$, $u_y = N(u_t, \varepsilon_y)$, $v_y = N(v_t, \varepsilon_y)$, and in addition normal distributed true components: $u_t = N(0, \sigma)$,

$v_t = N(0,\sigma)$, where $N(0, \sigma)$ indicates the normal distribution with zero mean and standard deviation σ. The wind speed distribution of system X, $p(f_x)\,df_x$, then becomes:

$$p(f_x)\,df_x = \frac{f_x}{\sigma_x^2}\exp[-\frac{f_x^2}{2\sigma_x^2}]\,df_x \qquad \textbf{(B1)}$$

where $\sigma_x^2 = \sigma^2 + \varepsilon_x^2$. A similar expression can be derived for system Y. The expected mean value of f_x will be $< f_x > = \sqrt{\pi/2}\,\sigma_x$, and $< f_x - f_y > = \sqrt{\pi/2}(\sigma_x - \sigma_y) \approx \sqrt{\pi/2}(\varepsilon_x^2 - \varepsilon_y^2)/\sigma$. Thus, the difference in mean wind speed is generally non-zero and a *pseudo* bias occurs, since the component error distributions were not biased. More detailed analysis shows that the *pseudo* bias results from the fact that the wind speed error distribution is asymmetric in case of symmetric wind component error distributions, especially for low wind speeds.

KNMI Technical report; TR-193

KNMI

European Space Agency Contract Report

Error modelling of scatterometer, *in-situ*, and ECMWF model winds; A calibration refinement

APPENDIX

(figures)

Author: Ad Stoffelen

ESA contract number: RFQ/AOP/WK/333193

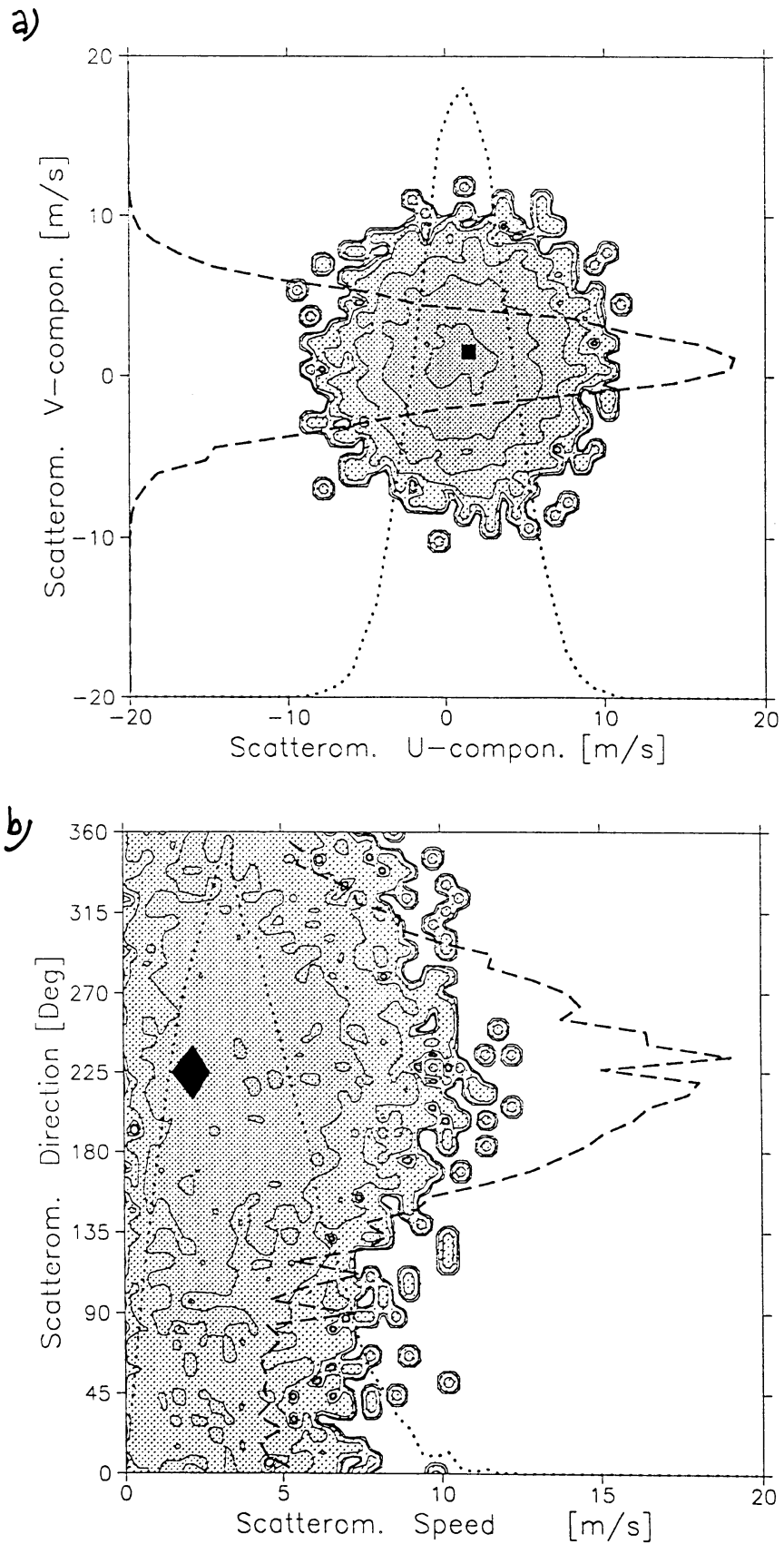

Figure 1: The distribution of scatterometer winds for ECMWF winds with component values in between 1.1 and 1.9 ms^{-1}. The distribution as a function of (a) the components and (b) as a function of speed and direction is shown. The ECMWF wind subdomain is indicated by a black box. The relative distribution of points (pdf) along the horizontal and vertical parameter axes are represented by the dotted and dashed lines respectively. Component errors are simpler to describe than speed and direction errors.

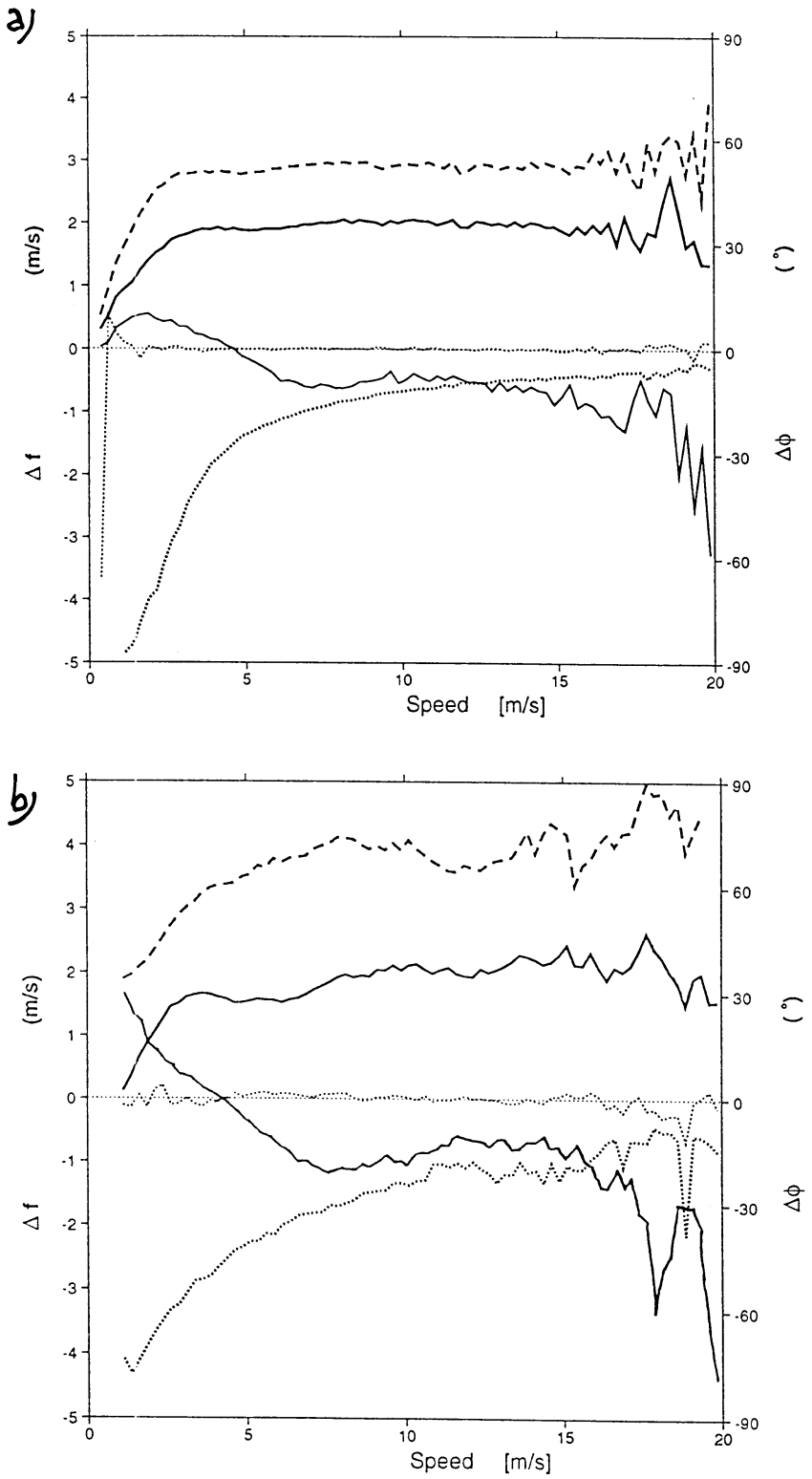

Figure 2: (a) simulated and (b) true wind speed and direction difference statistics of ECMWF model minus scatterometer as a function of average wind speed. (*Pseudo)* speed bias (thin solid), standard deviation (thick solid), direction bias (thin dotted), standard deviation (thick dotted), and vector RMS (dashed) of differences are shown. The simulation (a) is done with the scatterometer winds as "truth" and wind component standard errors of 1.0 and 1.8 ms^{-1} for the ECMWF model and scatterometer respectively. (b) is for the first node at the inner swath, which is the noisiest from all nodes. Although (b) is noisier, the general speed and direction error characteristics are well simulated in (a) by the wind component error model.

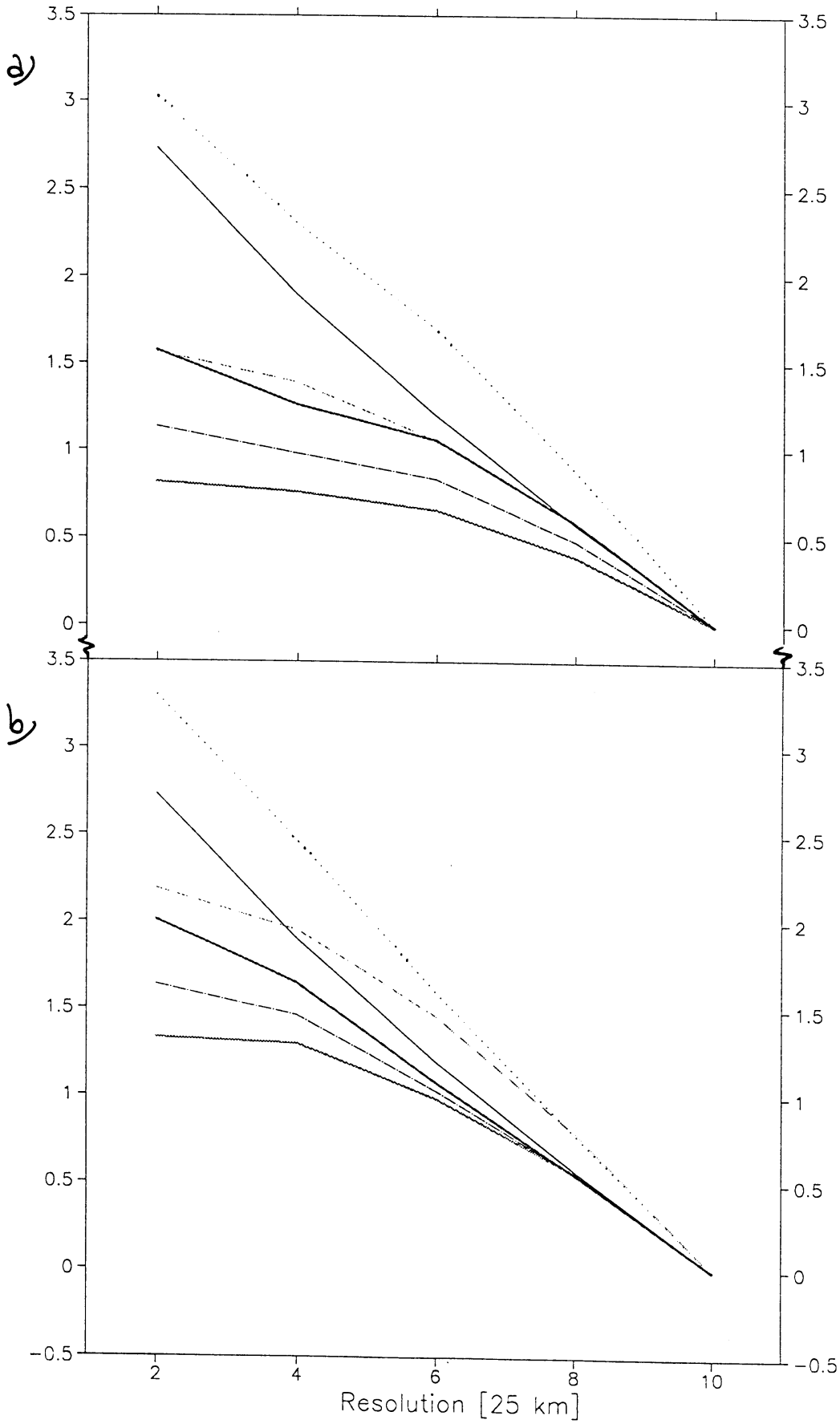

Figure 3: The reduction in true and error variance of scatterometer and ECMWF model for resolutions between 50 and 250 km (see text). In (a) the along-track ERS-1 component and in (b) the across-track component is shown. The scatterometer variance (thin dotted line), the ECMWF model variance (thin dashed line), their correlation (thin dash-dotted line), and the variance in a climatological spectrum (thin solid line) are drawn. An estimate of the resolved true variance by the scatterometer and the ECMWF model is represented respectively by the thick black and grey lines. The scatterometer better resolves the smaller scales.

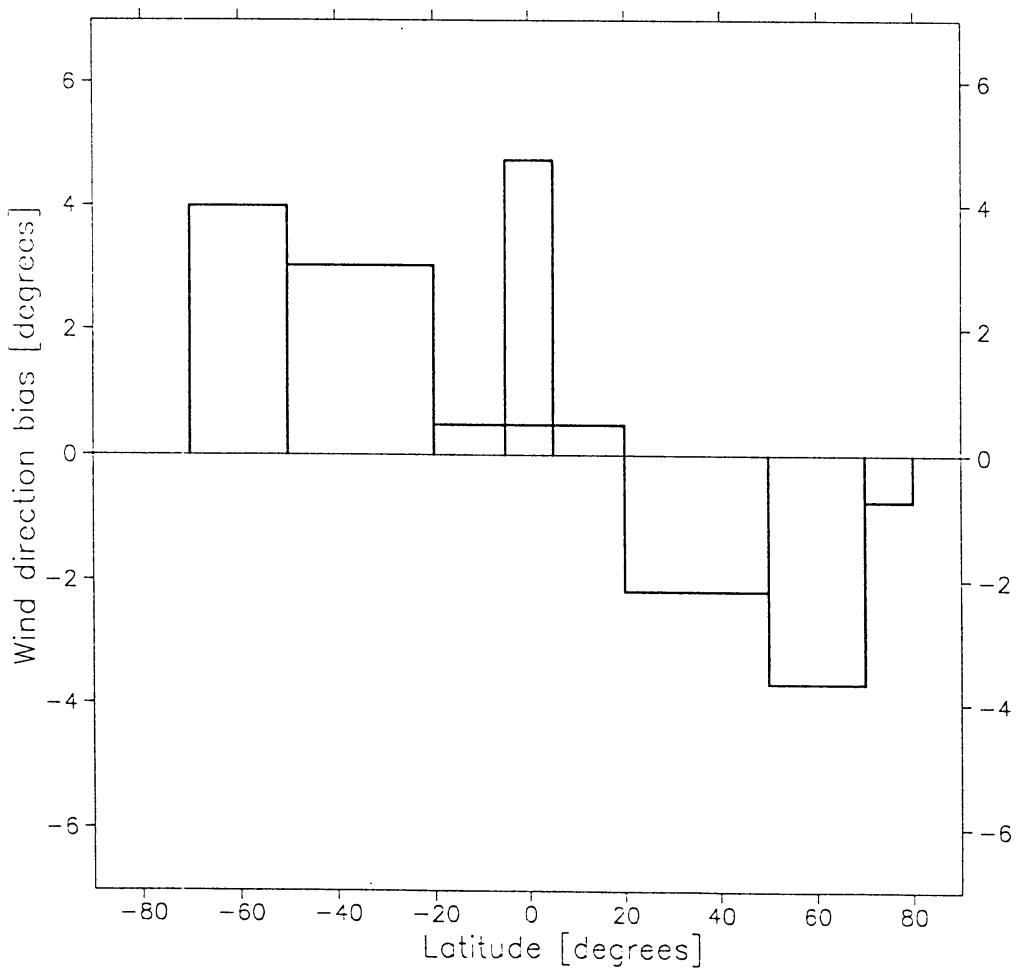

Figure 4: Scatterometer minus ECMWF model wind direction bias as a function of latitude. Data are from the period mid november to end december 1994. A scatterometer or ECMWF model bias exists at the equator and at the storm track latitudes.

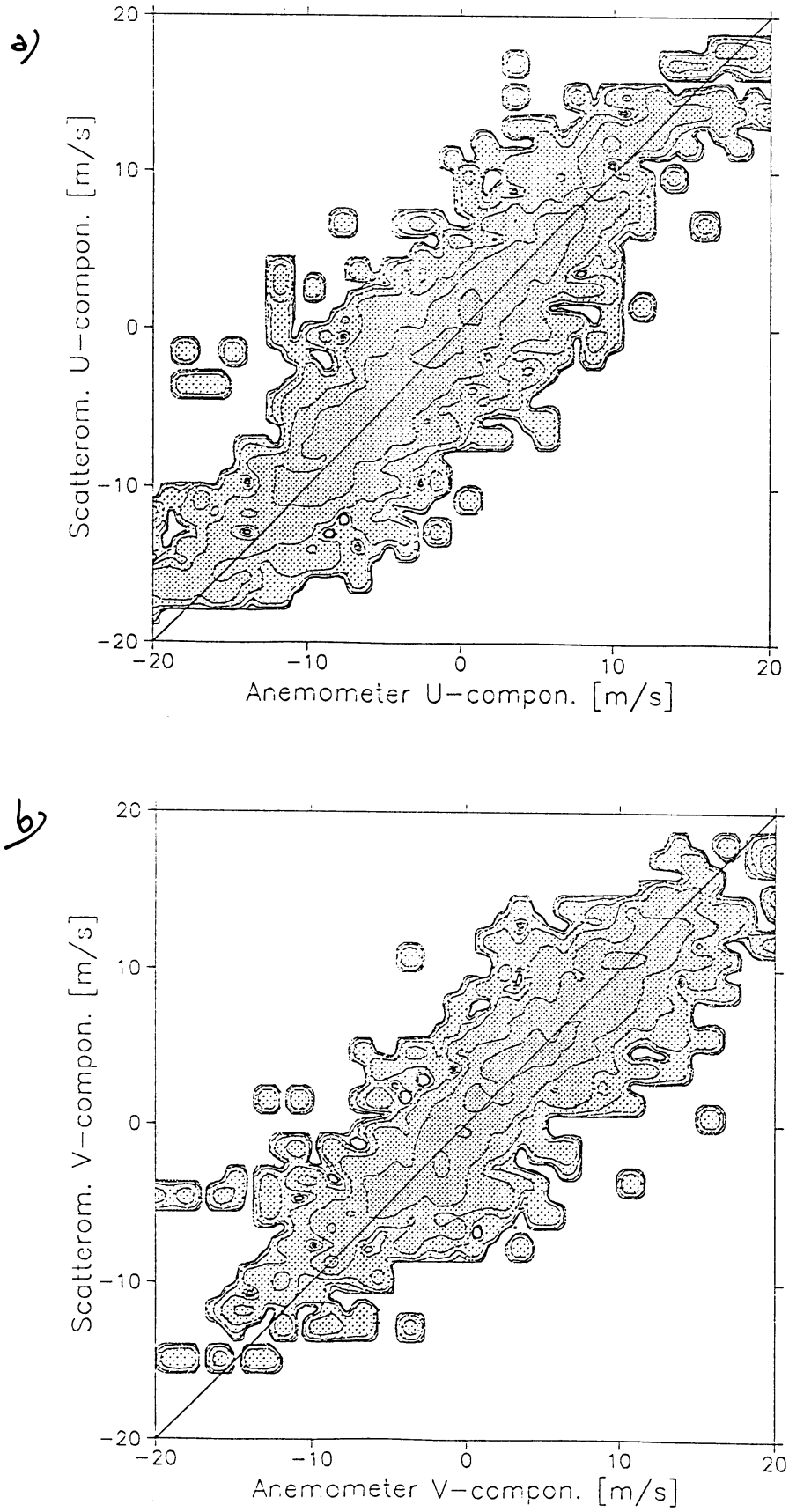

Figure 5: Joint distributions for the along-track (u) and across-track (v) ERS-1 wind components respectively for the (a-b) anemometer and scatterometer. (c-d) scatterometer and ECMWF model. and (e-f) ECMWF model and anemometer winds. These plots show in the wind domain the full characteristics of the triple collocation data base.

c)

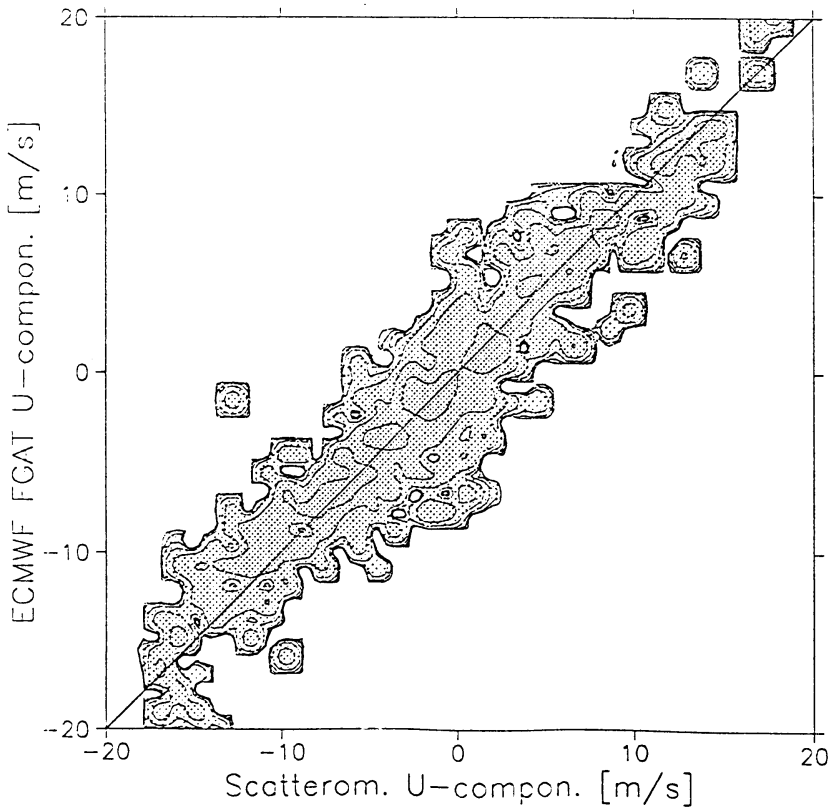
ECMWF FGAT U-compon. [m/s]
Scatterom. U-compon. [m/s]
20
10
0
-10
-20
-20
-10
0
10
20

d)

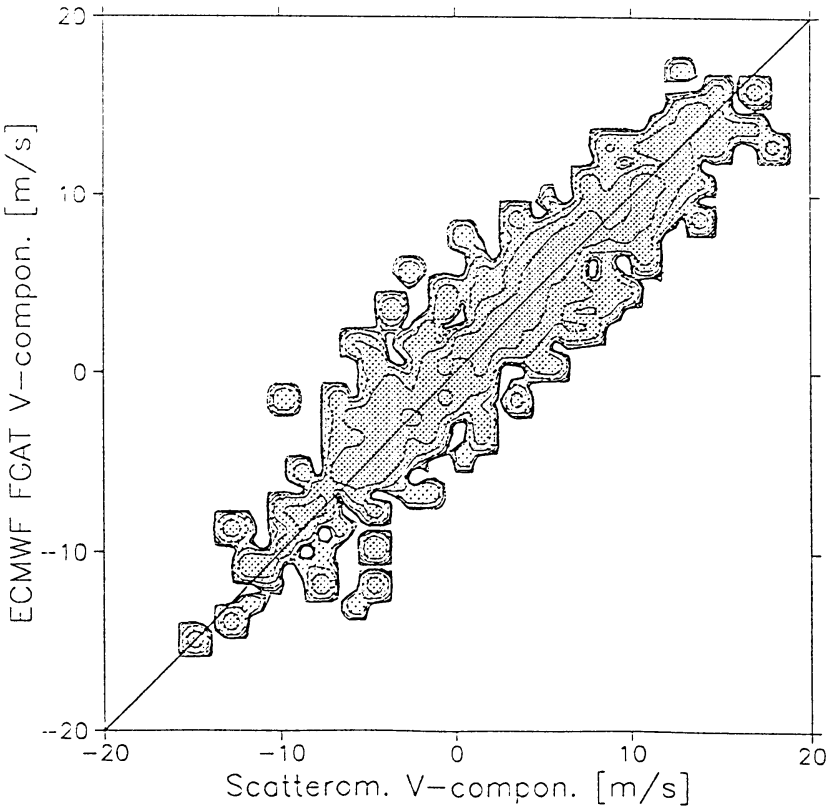
ECMWF FGAT V-compon. [m/s]
Scatterom. V-compon. [m/s]
20
10
0
-10
-20
-20
-10
0
10
20

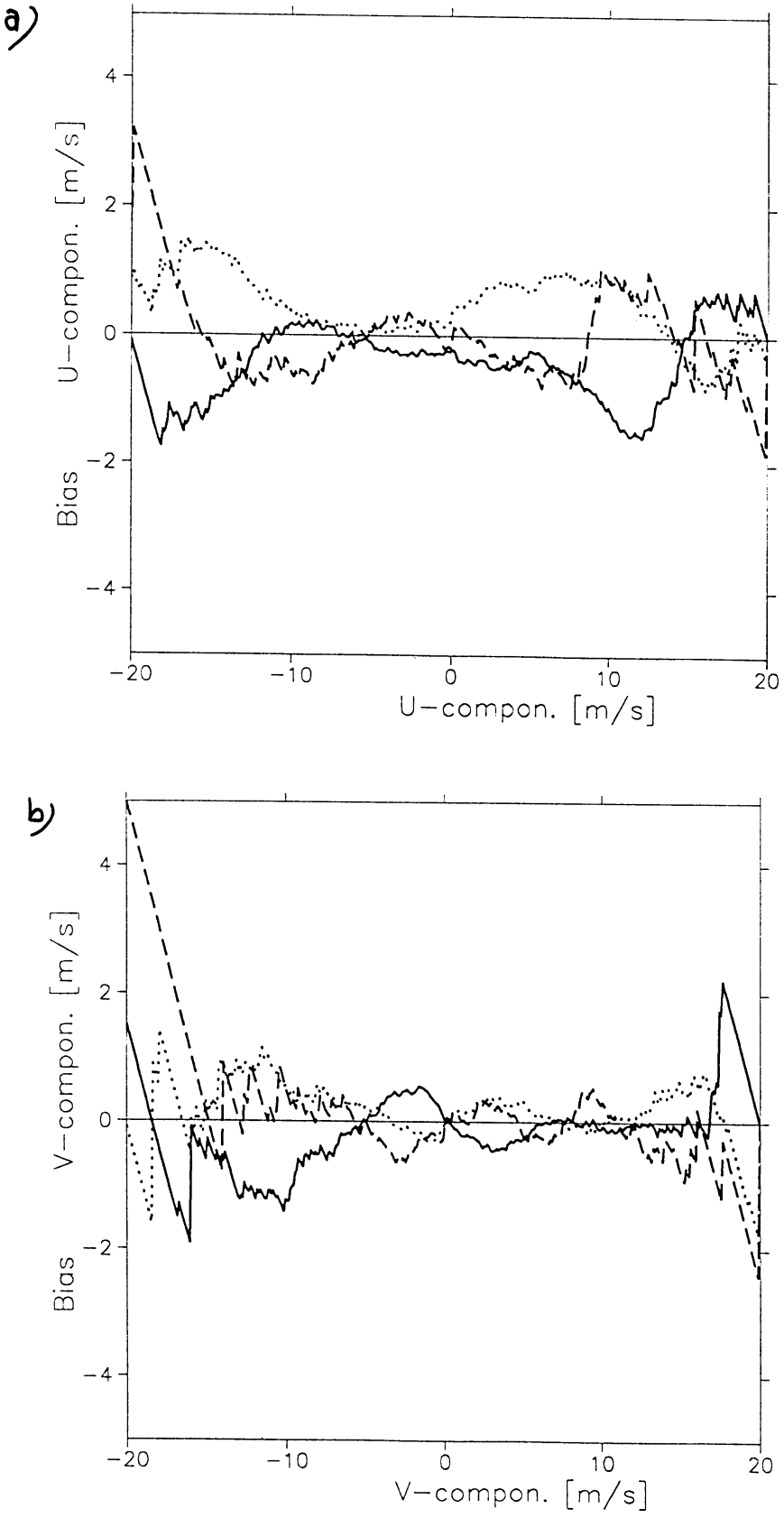

Figure 6: Higher order calibration by cumulative distribution mapping (see text) for (a) the along-track and (b) the across-track ERS-1 wind components. The biases of scatterometer with respect to anemometer (solid), ECMWF model with respect to scatterometer (dotted), and anemometer with respect to ECMWF model (dashed) winds are shown. Although large biases are present, there is no consistent correction apparent in the data.

e)

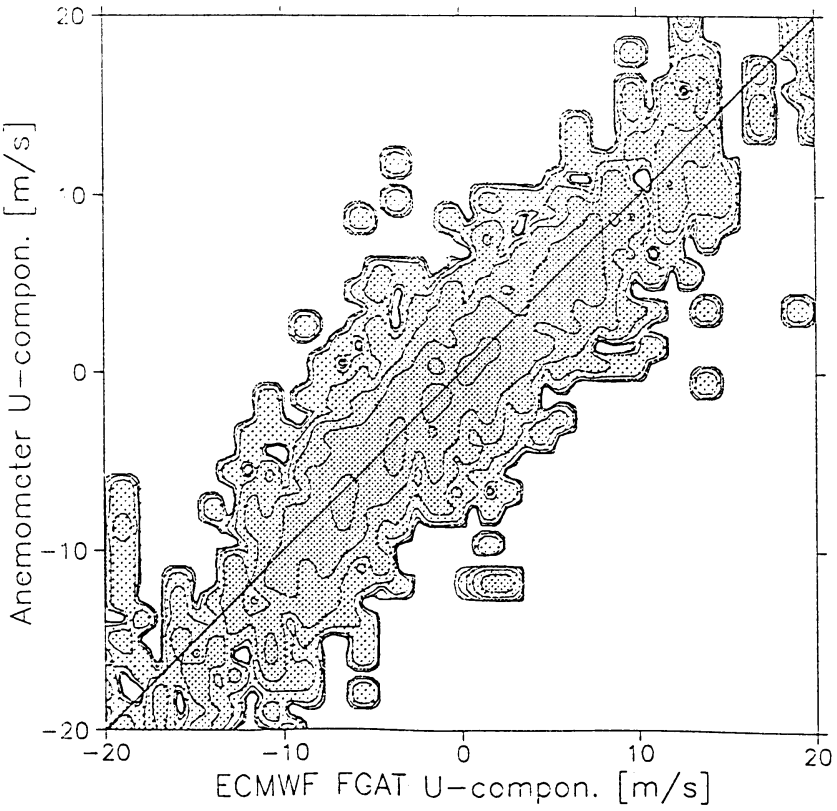
Anemomcter U-compon. [m/s]
ECMWF FGAT U-compon. [m/s]
20
10
0
-10
-20
-20
-10
0
10
20

f)

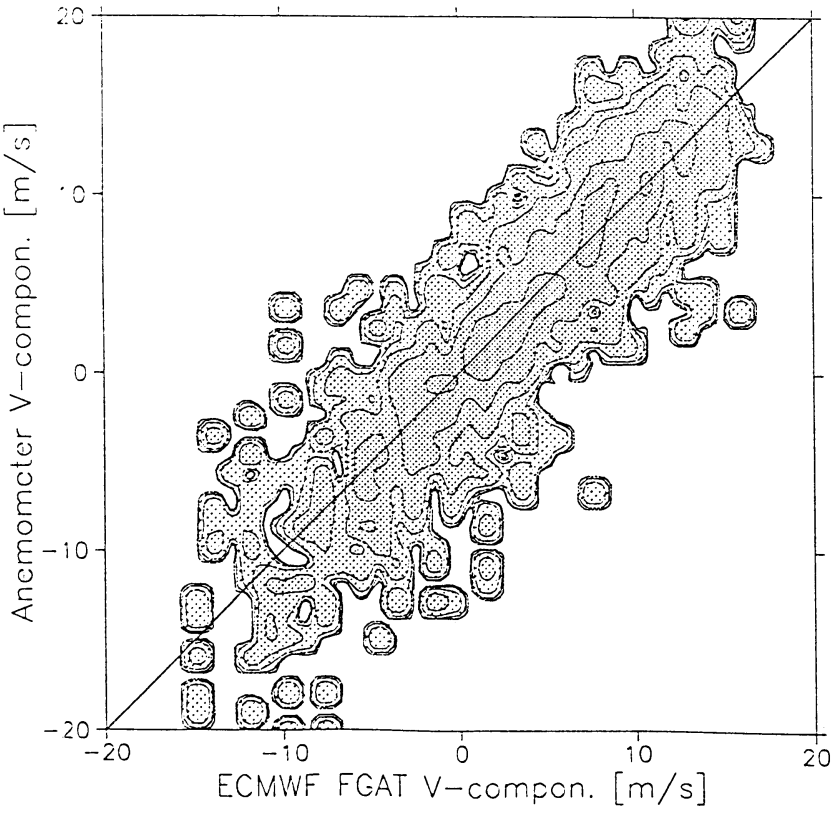
Anemomcter V-compon. [m/s]
ECMWF FGAT V-compon. [m/s]
20
10
0
-10
-20
-20
-10
0
10
20

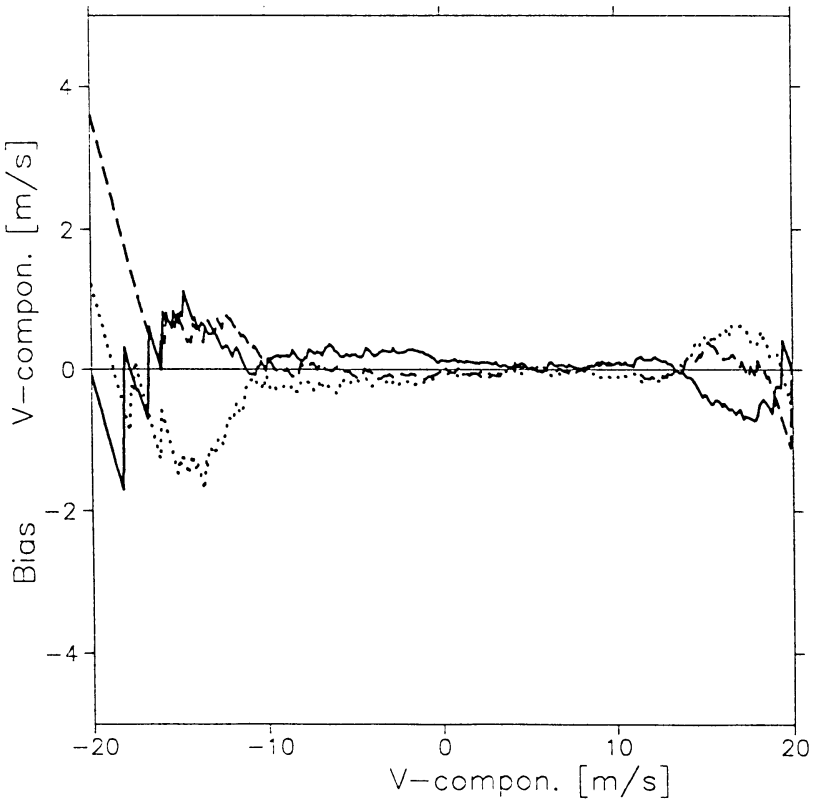

Figure 7: As figure 6, but for three simulated observation systems with a constant and normal error of zero mean and standard error of 2.5 ms^{-1}, 1.5 ms^{-1}, and 0.9 ms^{-1}, representing respectively the anemometer, scatterometer and ECMWF model across-track wind component. The distribution of ECMWF winds was taken to be the "true" distribution. Poor sampling results in *pseudo* biases, especially at high speeds (compare figure 6).